PLC-based LP_{11} mode rotator with curved trench structure devised from wavefront matching method

Yoko Yamashita, Shuntaro Makino, Takeshi Fujisawa, *Member*, *IEEE*, Nobutomo Hanzasa, Taiji Sakamoto, Takashi Matsui, Kyozo Tsujikawa, Fumihiko Yamamoto, Kazuhide Nakajima, Kunimasa Saitoh, *Member*, *IEEE*

***Abstract*— A compact and low-loss PLC-based mode rotator is proposed. The mode rotator with curved trench structure is designed based on the wavefront matching method, which is an optimization algorithm based on the beam propagation method. The proposed mode rotator is 45% in size (1.0 mm) and has lower loss (1/5) compared with the conventional structure that has a straight trench. Furthermore, the proposed mode rotator can achieve low mode crosstalk.**

***Index Terms*—Mode multi/demultiplexer, PLC, WFM method**

I. Introduction

Internet traffic has rapidly increased, and therefore, it is necessary to expand the transmission capacity per optical fiber . Mode division multiplexing (MDM) using few-mode fiber (FMF) is one of the key technology to expand the transmission capacity, in which different modes transmit individual signals [1]. To realize MDM transmission, mode multi/demutliplexers (MUX/ DEMUXs) are important components required to multiplex and demultiplex different modes. To date, various types of mode MUX/DEMUXs have been proposed based on free-space optics [2], fiber couplers [3-5], photonic lanterns [6], planar lightwave circuits (PLCs) [7-10], and so on. The PLC-based mode MUX/DEMUX has desirable characteristics such as compactness, low insertion loss, and mass productivity. In order to increase the multiplexed-mode number of PLC-based mode MUX/DEMUXs, it is necessary to excite the LP_{11b} mode. Here, we define the LP_{11a} mode as the mode that has two intensity peaks in the plane of the PLC and LP_{11b} mode as the mode that has two intensity peaks in the vertical direction. Although the LP_{11a} mode can be excited by using PLC-based asymmetric directional coupler (ADC) [7], the LP_{11b} mode cannot be excited due to the different field distribution in the vertical direction. Therefore, an LP_{11a}/LP_{11b} mode rotator has been proposed [10,11] to excite the LP_{11b} mode in PLC chip, as shown in Fig. 1. The mode rotator has an asymmetric waveguide cross section, and the LP_{11a} (LP_{11b}) mode launched into the mode rotator is converted to the LP_{11b} (LP_{11a}) mode, as shown in Fig. 1. By properly designing the trench, which makes the waveguide asymmetric, large mode conversion efficiency is obtained. To realize multiple-mode MUX/DEMUX, several mode rotators are used on one device. For example, for a six-mode multiplexer [9], two mode rotators are necessary. Therefore, a more compact and lower-loss mode rotator is required. To attain the best device performance, optimization algorithms can be used.

In this letter, a compact and low-loss mode rotator with curved trench structure is proposed. First, we used wavefront matching (WFM) method, which is an optimization algorithm for PLC-based optical devices, for a conventional mode rotator with a straight uniform trench. The optimized geometry has almost uniformly bent waveguide and uniform trench structure and the loss and the length are significantly reduced. Using this geometry, we devise a novel mode rotator with curved trench structure. The proposed mode rotator is 45% in size and has lower loss compared with the conventional one.

II. Design of Mode Rotator Based on WFM Method

Figure 1 shows the schematic of the conventional PLC-based mode rotator. It is composed of an asymmetric waveguide with a single trench. By properly selecting the trench design parameters, the orthogonal LP_{11} modes, shown in Fig. 2, whose propagation constants are β_1 and β_2, are equally excited when LP_{11a} (LP_{11b}) mode is launched into the waveguide. If the device length is a half beat-length of these two orthogonal modes as defined by the following equation

$$L = \frac{\pi}{|\beta_1 - \beta_2|}, \tag{1}$$

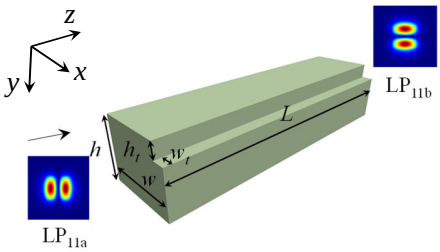

Fig. 1. Schematic of conventional mode rotator.

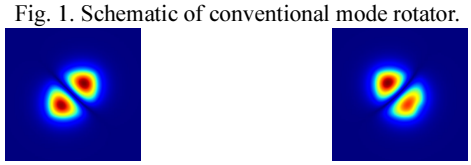

(a) (b)

Fig. 2. The two orthogonal modes of the mode rotator.

Manuscript received

Y. Yamashita, T. Fujisawa, S. Makino, and K. Saitoh are with the Graduate School of Information Science and Technology, Hokkaido University, Sapporo 060-0814, Japan (e-mail: yamashita@icp.ist.hokudai.ac.jp; fujisawa@ist.hokudai.ac.jp, makino@icp.ist.hokudai.ac.jp, ksaitoh@ist.hokudai.ac.jp,).

N. Hanzawa, T. Sakamoto, T. Matsui, K. Tsujikawa, F. Yamamoto, and K. Nakajima are with the Access Network Service Systems Laboratories, NTT Corporation, Tsukuba, Ibaraki 305-0805, Japan (e-mail: sakamoto.taiji@lab.ntt.co.jp).

the LP_{11a} (LP_{11b}) mode can be converted to the LP_{11b} (LP_{11a}) mode. Table I shows the design parameters of the conventional structure. The parameters of PLCs are the refractive-index difference, Δ = 1.0%; waveguide height, h = 10.0 μm; and waveguide widths, w = 10.1 μm. The trench parameters, w_t, h_t, and L are reported in [9]. The conventional mode rotator with these parameters has a conversion efficiency (CE) of −0.135 dB from LP_{11a} mode to LP_{11b} mode at a wavelength of 1550 nm. Here, the CE is defined as

$$CE = 10\log_{10}\frac{P_{out}}{P_{in}}. \qquad (2)$$

P_{in} and P_{out} are the normalized powers of input and output modes, respectively. In order to obtain the optimal design directly from the desired characteristics, several optimization methods have been used, for example, genetic algorithm [12], topology optimization [13], and the WFM method [14-17]. The WFM method is the optimization algorithm based on the beam propagation method (BPM) [18,19], and the optimum index profiles are determined from the ideal output field. The WFM method has been applied to the waveguide lens [14] and the multimode interferometer [15], and its validity and effectiveness have been demonstrated experimentally. Recently, we developed the WFM method for MDM devices, and an ultrabroadband ADC was experimentally realized [8].

In the WFM method, a coupling coefficient η between forward and backward propagation fields is evaluated as

$$\eta = \left|\iint \psi^*(z)\phi(z)dxdy\right|^2 \qquad (3)$$

where ψ is the ideal output field that propagates from output port to input port, ϕ is the input field that propagates from the input port to the output port, and the superscript * represents the complex conjugate.

When the refractive-index-distribution is changed, the coupling coefficient η' (corresponding to the refractive-index-distribution change) is expressed as

$$\eta' \cong \eta + 2k\Delta z\eta\frac{\iint \delta n_m \,\mathrm{Im}\left[\psi^*(z)\phi(z)\right]dxdy}{\int \psi^*(z)\phi(z)dxdy}. \qquad (4)$$

Here δn_m is the refractive index change at each step of the BPM.

From (4), it can be seen that if we change δn_m in proportion to $\mathrm{Im}[\psi^*(z)\phi(z)]$, the coupling coefficient can be improved. The BPM analysis with this waveguide width modulation is iterated until converged geometry is obtained. The details of the WFM method can be found elsewhere [8,14].

Figure 3 shows the mode conversion efficiency from the LP_{11a} mode to the LP_{11b} mode as a function of the number of iterations of the WFM method at a wavelength of 1550 nm. We optimized two structures with device length L of 2.29 and 1.15 mm, respectively. Here, L = 2.29 mm is the optimized length

TABLE I. Structural parameters of the conventional mode rotator.

Δ	h	w	w_t	h_t	L
1.0%	10.0 μm	10.1 μm	1.5 μm	2.4 μm	2.29 mm

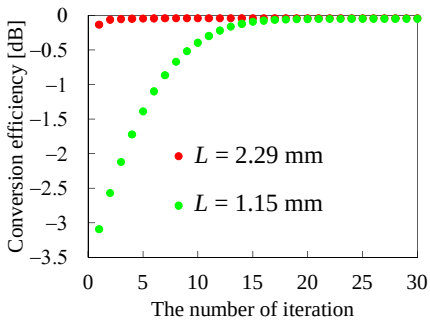

Fig. 3. LP_{11a}/LP_{11b} mode conversion efficiency as a function of the number of iteration of WFM method at wavelength of 1550 nm.

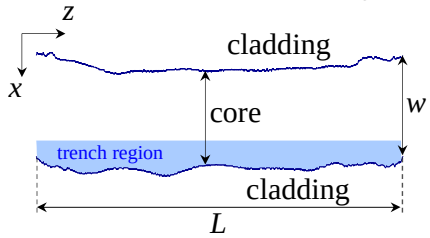

Fig. 4. Top-view of the WFM-optimized waveguide-core outline.

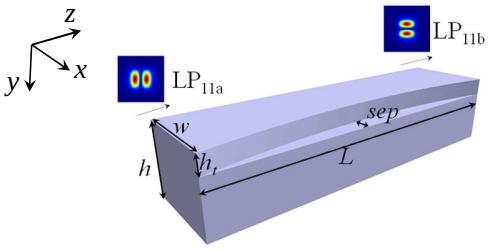

Fig. 5. Structure of the mode rotator with curved trench structure.

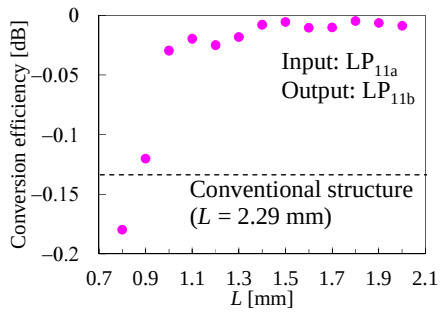

Fig. 6. Normalized output power of the LP_{11b} mode when the LP_{11a} mode is launched at wavelength of 1550 nm.

TABLE II. The structural parameters of the proposed mode rotator with curved trench structure.

L [mm]	h_t [μm]	sep [μm]
2.0	2.6	2.3
1.9	2.8	2.2
1.8	2.8	2.3
1.7	2.8	2.4
1.6	2.8	2.6
1.5	2.8	2.7
1.4	2.9	2.8
1.3	3.0	2.9
1.2	3.0	3.0
1.1	3.2	3.2
1.0	3.3	3.4
0.9	3.4	3.6
0.8	3.4	4.0

for LP_{11a}/LP_{11b} mode conversion for the conventional mode rotator, and the conversion efficiency is almost 100%. For L = 1.15 mm, the conversion efficiency is almost 50% (–3 dB) because the length is only half of the aforementioned structure. As shown in Fig. 3, the WFM method does not greatly improve the conversion efficiency of the rotator with L = 2.29 mm because the original structure has an efficiency of almost 100%. For L = 1.15 mm, the efficiency improvement is substantial. The efficiency increases from –3.09 dB to –0.047 dB after 25 iterations. The optimized efficiency is comparable to the L = 2.29 mm (–0.040 dB). Therefore, we can reduce the rotator size to approximately half by applying the WFM method while maintaining the efficiency. Figure 4 shows the top-view of the waveguide-core outline. Filled-blue region represents the trench region.

The overall waveguide is gently bent with small fluctuation in the waveguide width. The fluctuation is typical in WFM-optimized devices, and the period of the fluctuation seems to match with the beat length of LP_{01}/LP_{11a} mode leading to unintentional mode conversion between the LP_{11a} and the LP_{01} mode. The problems of this structure are 1) insertion loss caused by mode mismatch with connected waveguide and 2) unintentional LP_{11a}/LP_{01} mode crosstalk. Furthermore, there is an insertion loss between input waveguide without trench and rotator waveguide with trench. Then, we devise a new mode rotator with curved trench structure based on WFM-optimized structure in next section.

III. Mode Rotator with Curved Trench Structure

Based on WFM-optimized geometry shown in Fig. 4, a new mode rotator with curved trench structure is designed as presented in Fig. 5. In this structure, the waveguide itself is straight while the trench is curved. This structure is superior to the WFM-optimized structure shown in Fig. 4, because the main waveguide is not bent and there is no trench region at both ends. This structure can suppress insertion loss caused by mode mismatch with connected waveguide. The trench width has an adiabatic arch-shaped profile. The trench structure is defined as L (device length), Sep (the trench width at the center in z-direction), and h_t (trench height). The curve of the trench is a part of a circle with the following bent radius,

$$R = \frac{L^2 + 4sep^2}{8sep}. \quad (5)$$

The parameters of PLCs are the same of the conventional and WFM-optimized structures (Table I). Figure 6 shows the mode conversion efficiency from the LP_{11a} mode to the LP_{11b} mode as a function of L at a wavelength of 1550 nm. The trench parameters of Sep and h_t are optimized for each L as shown in Table II. It can be seen that the trench size becomes larger for shorter L, because it is necessary to increase the difference of propagation constants between LP_{11} orthogonal modes to decrease the device length. The dashed line in Fig. 6 shows the conversion efficiency of the conventional structure with L = 2.29 mm. From Fig. 6, it can be seen that the mode rotator with curved trench structure has better transmission than the conventional structure from L = 0.9 to 2.0 mm. For L = 1.0 mm, the length is 45% and the loss is 5 times lower compared with those of the conventional structure. In general, the size of PLC device is a few millimeters; therefore, the 1 mm reduction is very effective. In terms of fabrication, because PLC-based mode rotator with straight trench has already been fabricated [9], the proposed rotator with curved trench structure could be fabricated by the same process.

We evaluate the crosstalk (XT) to undesired modes for the LP_{11a} mode input, namely, the remaining power of LP_{11a} and LP_{01} modes at the output of the rotator. Figure 7 shows the XT to (a) the LP_{11a} mode and (b) the LP_{01} mode when the LP_{11a} mode is launched to the mode rotator at a wavelength of 1550 nm. Although the XT to LP_{01} mode is similar to that of the conventional structure (approximately –30 dB), the XT to the LP_{11a} mode is significantly reduced compared with the conventional mode rotator.

Figure 8 shows transmission of the LP_{01} mode when the LP_{01} mode is launched to the proposed mode rotator at a wavelength of 1550 nm. Because the mode rotator will be used along with ADCs to construct the MDM MUX [9], the loss of the LP_{01} mode should be small. From Fig. 8, we can say that the transmission of the LP_{01} mode can be improved by using a curved trench structure.

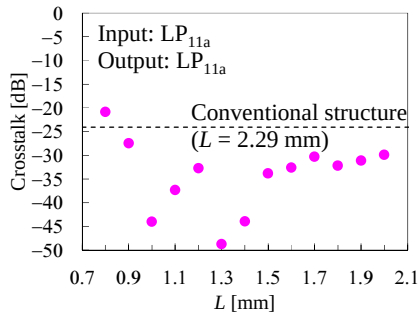

(a)

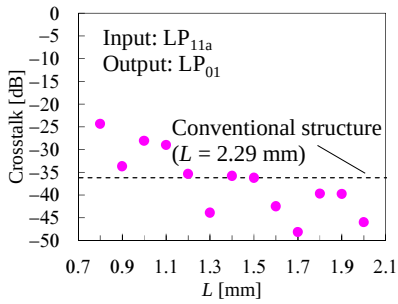

(b)

Fig. 7. Crosstalk to the (a) LP_{11a} and (b) LP_{01} modes when the LP_{11a} mode is launched at wavelength of 1550 nm.

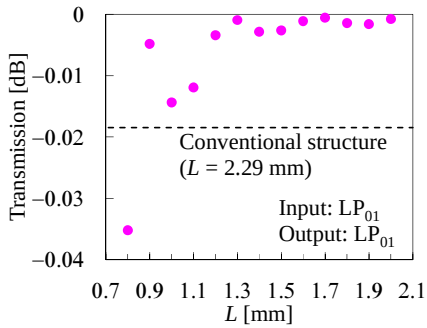

Fig. 8. Transmission of the LP_{01} mode when the LP_{01} mode is launched at wavelength of a 1550 nm.

Finally, wavelength dependence of the mode rotator is evaluated. Figure 9 shows the transmission spectra of (a) the mode conversion from the LP_{11a} mode to the LP_{11b} mode, (b) the modal XT, and (c) the transmission from the LP_{01} mode to the LP_{01} mode. The dashed and solid lines show the transmission of conventional and curved trench (L = 1.0 mm) structures, respectively. For the LP_{11b} mode input, similar characteristics are obtained as LP_{11a} mode is input. Because the structure has low polarization dependence, the wavelength dependence of LP_{11a} mode of x-pol is only shown in Fig. 9. As shown in Fig. 9, the curved trench structure has lower wavelength dependence, higher mode conversion efficiency, and smaller modal XT from 1.45 μm to 1.65 μm compared to the conventional structure, which shows the superiority of the proposed structure.

IV. Conclusion

A compact and low-loss PLC-based mode rotator was proposed. A mode rotator with a curved trench structure was devised based on the WFM method. The proposed mode rotator is 45% in size (1.0 mm) and has lower loss (1/5) compared with the conventional structure with a straight trench. Furthermore, the proposed mode rotator can achieve low mode crosstalk. For multi-mode multiplexers, the proposed low-loss and compact mode rotator device would be beneficial in the integration of PLC devices.

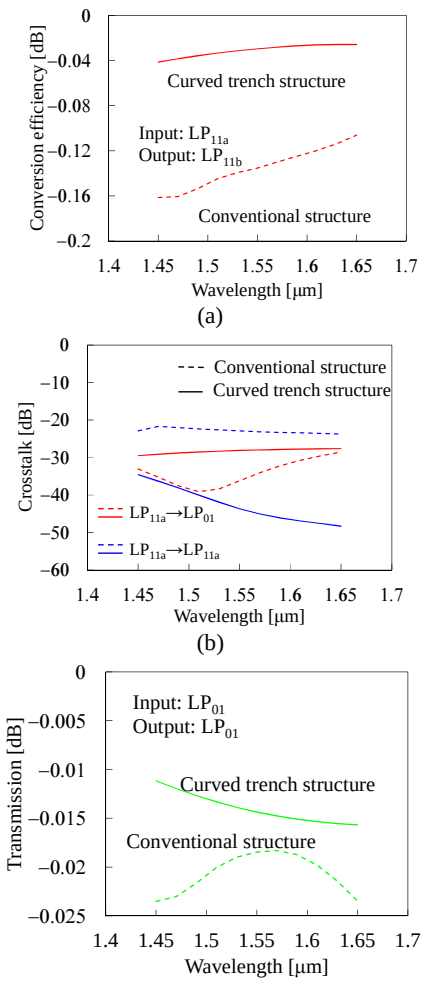

Fig. 9 Transmission spectra of (a) the mode conversion from the LP_{11a} mode to the LP_{11b} mode, (b) the unintentional mode crosstalk, and (c) the transmission from the LP_{01} mode to the LP_{01} mode.

References

[1] T. Morioka, Y. Awaji, R. Ryf, P. Winzer, D. Richardson, and F. P oletti, "Enhancing optical communications with brand new fibers," *IEEE Commun. Mag.*, vol. 50, no. 2, pp. s31–s42, Feb. 2012.

[2] E. Ip, N. Bai, Y.-K. Huang, E. Mateo, F. Yaman, M.-J. Li, S. Bickham, S. Ten, Y. Luo, G.-D. Peng, G. Li, T. Wang, J. Linares, C. Montero, and V. Moreno, "6x6 MIMO transmission over 50+25+10 km heterogeneous spans of few-mode fiber with inline erbium-doped fiber amplifier," *Optical Fiber Communication Conference*, OTu2C.4, 2012.

[3] J. D. Love and N. Riesen, "Mode-selective couplers for few-mode optical fiber networks," *Opt. Lett.*, vol. 37, no. 19, pp. 3990–3992, Oct. 2012.

[4] N. Hanzawa, K. Saitoh, T. Sakamoto, T. Matsui, S. Tomita, and M. Koshiba, "Mode-division multiplexed transmission with fiber mode couplers," *Optical Fiber Communication Conference*, OW1D.4, 2012.

[5] A. Li, J. Ye, X. Chen, and W. Shieh, "Low-loss fused mode coupler for few-mode transmission," *Optical Fiber Communication Conference*, OTu3G.4, 2013.

[6] S. G. Leon-Saval, N. K. Fontaine, J. R. S. Gil, B. Ercan, R. Ryf, and, J. Bland-Hawthorn, "Mode-selective photonic lanterns for space-division multiplexing," *Opt. Express*, vol. 22, no. 1, pp. 1-9, Jan. 2014.

[7] N. Hanzawa, K. Saitoh, T. Sakamoto, T. Matsui, K. Tsujikawa, M. Koshiba, and F. Yamamoto, "Two-mode PLC-based mode multi/demultiplexer for mode and wavelength division multiplexed transmission," *Opt. Express*, vol. 21, no. 22, pp. 25752–25760, Nov. 2013.

[8] Y. Yamashita, T. Fujisawa, S. Makino, N. Hanzawa, T. Sakamoto, T. Matsui, K. Tsujikawa, F. Yamamoto, K. Nakajima, and K. Saitoh, "Design and fabrication of broadband PLC-based 2-mode multi/demultiplexer using wavefront matching method," *J. Lightw. Technol.*, http://ieeexplore.ieee.org/document/7790852/, 2016.

[9] K. Saitoh, N. Hanzawa, T. Sakamoto, T. Fujisawa, Y. Yamashita, T. Matsui, K. Tsujikawa, K. Nakajima, "PLC-based mode multi/demultiplexers for mode division multiplexing," *Opt. Fiber Technol.*, vol. 35, pp.80-02, Feb. 2017..

[10] K. Saitoh, T. Uematsu, N. Hanzawa, Y. Ishizaka, K. Masumoto, T. Sakamoto, T. Matsui, K. Tsujikawa, and F. Yamamoto, "PLC-based LP11 mode rotator for mode-division multiplexing transmission," *Opt. Express*, vol. 22, no. 16, pp. 19117–19130, Aug. 2014.

[11] J. Wang, D. Zhao, J. Xu, X. Xue, and X. Zhang, "High-Order Mode Rotator on the SOI Integrated Platform," *IEEE Photon. J.*, vol. 8, no. 2, pp. 6500308–6500308, Apr. 2016.

[12] B. R. West and S. Honkanen, "MMI devices with weak guiding designed in three dimensions using a genetic algorithm," *Opt. Express*, vol. 12, no. 12, pp. 2716–2722, Jun. 2004.

[13] Y. Tsuji and K. Hirayama, "Design of optical circuit devices using topology optimization method with function-expansion- based refractive index distribution," *IEEE Photon. Technol. Lett.*, vol. 20, no. 12, pp. 982–984, Jun. 2008.

[14] T. Hashimoto, T. Saida, I. Ogawa, M. Kohtoku, T. Shibata, and H. Takahashi, "Optical circuit design based on a wavefront-matching method," *Opt. Lett.*, vol. 30, no. 19, pp. 2620–2622, Oct. 2005.

[15] Y. Sakamaki, T. Saida, T. Hashimoto, and H. Takahashi, "New optical waveguide design based on wavefront matching method," *J. Lightw. Technol.*, vol. 25, no. 11, pp. 3511–3518, Nov. 2007.

[16] T. Fujisawa, T. Kitoh, K. Watanabe, K. Suzuki, M. Kotoku, and H. Takahashi, "Wide-bandwidth, low-waveguide-width-sensitivity InP-based multimode interference coupler designed by wavefront matching method," *IEICE Electron. Express*, vol. 8, no. 24, pp. 2100–2105, Dec. 2011.

[17] K. Saitoh and M. Koshiba, "Approximate scalar finite-element beam propagation method with perfectly matched layers for anisotropic optical waveguides," *J. Lightw. Technol.*, vol. 19, no. 5, pp. 786–792, May 2001.

[18] T. Fujisawa and M. Koshiba, "Full-vector finite-element beam propagation method for three-dimensional nonlinear optical waveguides," *J. Lightw. Technol.*, vol. 20, no. 10, pp. 1876–1884, Oct. 2002.